The 2010 IEEE/RSJ International Conference on
Intelligent Robots and Systems
October 18-22, 2010, Taipei, Taiwan

Control of a powered planar biped without ankle actuation

Ryuta Ozawa and Yoshimasa Kojima

Abstract— **This paper introduces a control method for a powered planar biped without ankle actuation. The existence of an ideal slope, on which the biped can walk without actuation, is assumed. The proposed controller can realize stable walking, as if the biped were on an ideal slope when the biped is on a different slope. The proposed controller has no singular points, whereas the control input diverges to infinity, unlike conventional controllers for powered passive walkers. Selected simulations were executed with a simple compass-like biped and a four-link biped with a mass body to validate the effectiveness of the proposed controller.**

I. INTRODUCTION

Many researchers have been studying passive dynamic walkers, which can walk down a shallow slope without any actuation, after the pioneering work of McGeer [1]. The fundamental concept governing these walkers is that the energy consumed by foot impact is recovered by the gravitational potential. Some researchers have been trying to extend this method to powered walking on level ground [2], [3], [4], [5], because passive walkers are much more efficient than conventional powered bipedal robots, even if it is powered [5], [6], [7].

Goswami et al. [2] designed an energy feedback controller to provide a robot with energy via actuation. They fed back the current energy to track the desired energy. They considered ankle drive to be an unrealistic assumption for the modeling of a compass-like biped and instead applied their algorithm to a biped with hip actuation only. It is difficult to control walking velocity using this algorithm. As such, they added a velocity compensation term into the desired energy formula to facilitate better control of walking velocity [8]. The drawbacks of this control algorithm are that the control input is divided by the relative velocity between the swing and stance legs, and the input tends toward infinity as the velocity approaches zero.

Spong [3] proposed a passivity-based controller with gravity compensation to realize the walking dynamics that would occur on the ideal slope, while on level ground. This controller required multi-joint actuation, including the ankle joint. Thus, it is difficult to apply this method to robots without feet. Spong discussed the treatment of under-actuated bipeds but it is an irregular treatment based on Goswami's work [2]. Spong [9] extended the two-dimensional passivity-based controller to the three dimensional biped using the concept of controlled symmetry. Asano et al. [4] proposed virtual gravity control for a fully actuated compass-like biped. They compensated the horizontal potential energy to realize 'virtual gravity' on level ground. They used ankle actuation because a lot of walking robots, which are based on a zero moment point (ZMP), use this actuation scheme. However, passive walkers use rocker functions [10] instead of foot contact with the ground at a point. In this case, it is difficult to model the robot as a biped with ankle actuation [1], [11], [12], [13]. The ankle actuation also may require a heavy foot or implausible torques due to ground contact.

For a biped without feet, Chevalleau et al. [14] designed a walking controller based on hybrid zero dynamics and virtual constraints to realize control of a bipedal walker without taking ZMP into account. This method forces a robot to follow a virtual constraint and seems to require more energy than control methods based on passive walking dynamics.

This paper proposes a gravity compensation method for a two dimensional biped without ankle actuation. This method is based on virtual gravity concept (e.g., [3] [4]) to realize stable walking on a shallow slope.

There are two advantages compared with the existing powered biped with virtual gravity. First, this method can be applied to bipeds with point feet, and the proposed controller does not have any terms that are divided by the relative velocity between the legs as in [2], [4] so that the control input does not diverge to infinity at singular points. Second, it is easy to execute the proposed controller, because it uses only the Jacobian and the gravitational forces to calculate the control input.

Section II describes the dynamics of the robot to account for the constraint between the foot and the ground. Section III proposes a control method to compensate the gravity effect on an ideal slope. In section IV, some simulations are executed to confirm the validity of the controller with a simple compass-like biped and a four-link biped with a mass body in a plane. Section V concludes this paper.

II. MODELING OF A WALKING BIPED

Fig. 1 shows a physical model of a biped in a plane. We assume that this robot has no foot link, and the body is modeled as a link, whose center of mass is at the hip joint.

Let $\boldsymbol{x} = (x, y)^{\mathrm{T}} \in R^2$ be the position of the upper body with respect to the fixed coordinates on the ground. Let $\boldsymbol{q} = (\boldsymbol{q}_1^{\mathrm{T}}, \boldsymbol{q}_2^{\mathrm{T}})^{\mathrm{T}} \in R^{N_1+N_2}$ be the joint angle of both legs.

Then, the state of the system can be expressed as $\boldsymbol{z} = (\boldsymbol{x}^{\mathrm{T}}, \boldsymbol{q}^{\mathrm{T}})^{\mathrm{T}} \in R^N$, where $N = 2 + N_1 + N_2$. The contact between the foot and the ground is at a point. The following assumptions are made [15]; 1) friction between the foot and the ground is large enough to prevent the foot from slipping,

This work was not supported by any organization

R. Ozawa is with Dept. of Robotics, School of Science and Technology, Ritsumeikan University, 535-8577 Shiga, Japan ryuta@se.ritsumei.ac.jp

Y. Kojima is with Disco corporation, 143-8580 Tokyo, Japan

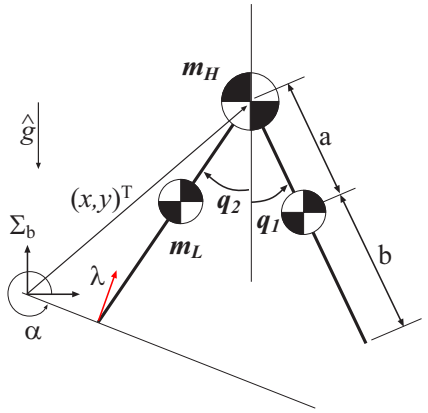

Fig. 1. A walking robot on a slope

2) the swing and stance legs can be changed instantaneously, and 3) the collision between the ground and the foot is perfectly inelastic. When the i th leg supports the body, the constraint between the leg and the ground can be described as follows:

$$\boldsymbol{f}_i(\boldsymbol{z}) = \boldsymbol{0}. \tag{1}$$

The time derivative of the constraint is calculated as

$$\boldsymbol{J}_i(\boldsymbol{z})\dot{\boldsymbol{z}} = \begin{cases} \begin{pmatrix} \boldsymbol{I}_M & \boldsymbol{J}_{s1}(\boldsymbol{q}) & \boldsymbol{0} \end{pmatrix} \dot{\boldsymbol{z}} = \boldsymbol{0} & \text{if } i = 1, \\ \begin{pmatrix} \boldsymbol{I}_M & \boldsymbol{0} & \boldsymbol{J}_{s2}(\boldsymbol{q}) \end{pmatrix} \dot{\boldsymbol{z}} = \boldsymbol{0} & \text{if } i = 2. \end{cases} \tag{2}$$

Let $\boldsymbol{H}(\boldsymbol{z})$ be the inertia matrix of the robot and $U_r(\hat{\boldsymbol{a}}, \boldsymbol{z})$ be the potential energy generated by the acceleration vector $\hat{\boldsymbol{a}}$. Then the equation of motion (EOM) of the robotic system is described as follows (e.g., [16]):

$$\begin{aligned} \boldsymbol{H}(\boldsymbol{z})\ddot{\boldsymbol{z}} + \left\{ \frac{1}{2}\dot{\boldsymbol{H}}(\boldsymbol{z}) + \boldsymbol{S}(\boldsymbol{z}, \dot{\boldsymbol{z}}) + \boldsymbol{C} \right\} \dot{\boldsymbol{z}} + \boldsymbol{g}(\boldsymbol{z}) \\ - \boldsymbol{J}_i^{\mathrm{T}}(\boldsymbol{z})\boldsymbol{\lambda} = \boldsymbol{A}^{\mathrm{T}}\boldsymbol{u}, \end{aligned} \tag{3}$$

where $\boldsymbol{S}(\boldsymbol{z}, \dot{\boldsymbol{z}})$ is the skew-symmetric matrix, $\boldsymbol{C}$ is the damping matrix, $\boldsymbol{\lambda} \in R^2$ is the ground reaction forces at the stance heel, $\boldsymbol{A}$ is the coefficient matrix and $\boldsymbol{u} = (\boldsymbol{u}_1, \boldsymbol{u}_2)^{\mathrm{T}} \in R^{N_1+N_2}$ is the controlled torque for both legs, and the gravitational vector is defined as

$$\boldsymbol{g}(\boldsymbol{z}) = \frac{\partial U_r(\hat{\boldsymbol{g}}, \boldsymbol{z})}{\partial \boldsymbol{z}}^{\mathrm{T}}, \tag{4}$$

where $\hat{\boldsymbol{g}}$ is the gravity acceleration. There is no actuator for controlling the upper body directly, therefore

$$\boldsymbol{A} = \begin{pmatrix} \boldsymbol{0} & \boldsymbol{I}_{N_1+N_2} \end{pmatrix} \in R^{N \times (N_1+N_2)}. \tag{5}$$

The key feature of this model is the lack of ankle joints. For example, with this model the compass-like biped has two control inputs on the hip, although the typical compass-like biped has one hip and two ankle inputs [2].

Next the collision between the foot and the ground was considered. The superscripts "$-$" and "$+$" express the state just before and after the contact. The contact is inelastic, thus,

$$\boldsymbol{J}_j(\boldsymbol{z})\dot{\boldsymbol{z}}^+ = \boldsymbol{0}. \tag{6}$$

The configuration was assumed to be unchanged during ground contact. Momentum is preserved as follows:

$$\boldsymbol{H}(\boldsymbol{z})\dot{\boldsymbol{z}}^- + \boldsymbol{J}_j^{\mathrm{T}}(\boldsymbol{z})\boldsymbol{\mu} = \boldsymbol{H}(\boldsymbol{z})\dot{\boldsymbol{z}}^+, \tag{7}$$

where $\boldsymbol{\mu}$ is the impulse of the contact forces at heel strike. Then, from eqs. (6) and (7), the velocity after the collision is given as follows:

$$\dot{\boldsymbol{z}}^+ = \left\{ \boldsymbol{I}_{M+N} - \boldsymbol{H}^{-1}\boldsymbol{J}_j^{\mathrm{T}} [\boldsymbol{J}_j \boldsymbol{H}^{-1} \boldsymbol{J}_j^{\mathrm{T}}]^{-1} \boldsymbol{J}_j^{\mathrm{T}} \right\} \dot{\boldsymbol{z}}^-. \tag{8}$$

We can express the next phase of walking using the EOM (3) by changing the Jacobian matrix $\boldsymbol{J}_i$, which implies the exchange of the stance and swing legs by using the new state $\boldsymbol{z}, \dot{\boldsymbol{z}}^+$.

III. Controller Design

In this section, we propose and explain the physical meaning of a controller that performs gravity compensation of a biped robot without ankle actuation, based on Spong's work [3].

Fig. 2 shows the image of the system. We assume that there is an ideal slope on which a biped robot can walk without any actuation. However, the current slope is not ideal. We would like the biped to walk as if it were on the ideal slope.

Let $\hat{\boldsymbol{g}}_{\mathrm{des}}$ be the gravitational acceleration vector when the robot is on the ideal slope. Then, the ideal gravitational force vector is given as follows:

$$\boldsymbol{g}_{\mathrm{d}}(\boldsymbol{z}) = \frac{\partial U_r(\hat{\boldsymbol{g}}_{\mathrm{des}}, \boldsymbol{z})}{\partial \boldsymbol{z}}^{\mathrm{T}}, \tag{9}$$

For example, let α be the angle of the current slope and β be the angle of the desired level ground as shown in Fig. 2. Then,

$$\hat{\boldsymbol{g}}_{\mathrm{des}} = -g_r \begin{pmatrix} -\sin(\beta - \alpha) \\ \cos(\beta - \alpha) \end{pmatrix}, \tag{10}$$

where g_r is the gravitational acceleration constant. $\hat{\boldsymbol{g}}_{\mathrm{des}}$ is not limited to the form in Eq. (10), and we can use any $\hat{\boldsymbol{g}}_{\mathrm{des}}$ to realize the stable slope walk. For example, see [4] as another candidate.

Let $\boldsymbol{g}_{\mathrm{in}}$ be the controlled gravitational force to generate the ideal gravitational force vector. Then,

$$\boldsymbol{g}_{\mathrm{in}} = -\boldsymbol{g}_{\mathrm{d}} + \boldsymbol{g}. \tag{11}$$

If the biped is full-actuated, then we can use $\boldsymbol{u} = \boldsymbol{A}^{-\mathrm{T}}\boldsymbol{g}_{\mathrm{in}}$, and the closed dynamic becomes

$$\begin{aligned} \boldsymbol{H}(\boldsymbol{z})\ddot{\boldsymbol{z}} + \left\{ \frac{1}{2}\dot{\boldsymbol{H}}(\boldsymbol{z}) + \boldsymbol{S}(\boldsymbol{z}, \dot{\boldsymbol{z}}) + \boldsymbol{C} \right\} \dot{\boldsymbol{z}} + \boldsymbol{g}_{\mathrm{d}}(\boldsymbol{z}) \\ - \boldsymbol{J}_i^{\mathrm{T}}(\boldsymbol{z})\boldsymbol{\lambda} = \boldsymbol{0}. \end{aligned} \tag{12}$$

This expresses the dynamics of the biped on the ideal slope. However, it is impossible to use the above control input because there is no control input to the upper body. Thus,

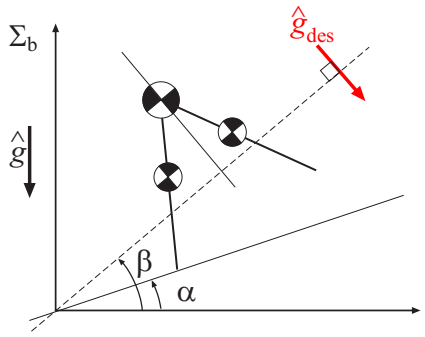

Fig. 2. powered simple biped walking

we need to compensate the input in a different way. To do this, $\boldsymbol{g}_{\text{in}}$ is described as follows:

$$\boldsymbol{g}_{\text{in}} = \begin{pmatrix} \boldsymbol{g}_b^{\text{in}} \\ \boldsymbol{g}_1^{\text{in}} \\ \boldsymbol{g}_2^{\text{in}} \end{pmatrix}, \tag{13}$$

where $\boldsymbol{g}_b^{\text{in}} \in R^2$ is the gravitational force vector acted on the upper body, and $\boldsymbol{g}_i^{\text{in}} \in R^{N_i} (i = 1, 2)$ is the gravitational force vector acted on the i th leg.

Here, we consider the roles of the swing and stance legs separately. The main difference between the stance and the swing legs is that the stance leg has to support the body. Thus, we will use the stance leg to compensate $\boldsymbol{g}_b^{\text{in}}$. The control input for the i th leg is defined as follows:

$$\boldsymbol{u}_i = \begin{cases} -\boldsymbol{J}_{si}^{\text{T}} \boldsymbol{g}_b^{\text{in}} + \boldsymbol{g}_i^{\text{in}} & \text{if the } i \text{ th leg supports the body.} \\ \boldsymbol{g}_i^{\text{in}} & \text{if the } i \text{ th leg is the swing leg.} \end{cases} \tag{14}$$

where $\boldsymbol{J}_{si}$ is the sub-matrix in the Jacobian matrix of Eq. (2). The control input never diverges at singular points, as shown in [2], [4], because it is not divided by a velocity term. In addition, the control input does not include any ankle actuation, as in [3], [4].

The following serves as an explanation of the meaning of the control input. From Eq. (2), the upper body velocity $\dot{\boldsymbol{x}}$ can be expressed as

$$\dot{\boldsymbol{x}} = -\boldsymbol{J}_{si} \dot{\boldsymbol{q}}_i. \tag{15}$$

Then, the power provided to the biped is

$$\begin{aligned} \sum_{j=1,2} \dot{\boldsymbol{q}}_j^{\text{T}} \boldsymbol{u}_j &= -\dot{\boldsymbol{q}}_i^{\text{T}} \boldsymbol{J}_{si}^{\text{T}} \boldsymbol{g}_b^{\text{in}} + \sum_{j=1,2} \dot{\boldsymbol{q}}_j^{\text{T}} \boldsymbol{g}_j^{\text{in}} \\ &= \dot{\boldsymbol{x}}^{\text{T}} \boldsymbol{g}_b^{\text{in}} + \sum_{j=1,2} \dot{\boldsymbol{q}}_j^{\text{T}} \boldsymbol{g}_j^{\text{in}} = \dot{\boldsymbol{z}}^{\text{T}} \boldsymbol{g}_{\text{in}}. \end{aligned} \tag{16}$$

This means that the power provided to the biped is equivalent to the power provided by gravitational force $\boldsymbol{g}_{\text{in}}$. Thus, the biped can walk as if it were on the ideal slope.

IV. Simulation

In this section we execute simulations using a planar compass-like biped and a planar four-link biped with a mass body.

A. In the case of the compass-like biped

We execute two simulations in this subsection: the unpowered simple biped on the ideal slope and the powered biped on level ground. The powered biped is controlled with the proposed controller. We can confirm the validity of our control method by comparing the results of these two simulations.

The parameters of the biped used in this simulation are shown in Table I. Fig. 3 (a) shows the phase graph of the unpowered biped when it walks down on a slope, whose angle is $\alpha = -0.03$ (rad). The left graph shows the phase graph of the hip joint in the transition, and the right graph shows that in the steady states after 7.5 (s). The pink and blue lines are the stance and swing legs in their initial configurations, respectively. The circles in the graph are the initial states. The upper and lower arcs show the swing and stance phases, respectively. The sharp edges of the right and left bottom in the figure are at the time of the foot contact and foot off, respectively. We can see that the trajectories of both legs are the same in steady state.

Fig. 3 (b) shows the phase graph of the powered biped walking on level ground ($\alpha = 0.0$ (rad)). The initial conditions are given to be equivalent to the unpowered case, and the ideal angle is designed as $\beta = -0.03$ (rad). The shapes of Fig. 3 (b) is almost the same as in Fig. 3 (a). Thus, the proposed method can realize the ideal gravitational force.

Fig. 4 shows the total energy of the unpowered biped. The sudden change of energy is caused by the impact between the foot and the ground. In the steady state, the energy provided by gravity is balanced by the energy lost through impact. We can see that the walking pattern becomes stable.

Fig. 5 (a) shows the control input of the powered biped. The pink and the blue lines are the control inputs for the first and second legs, respectively. The control inputs do not show any divergence at the singular points. The control input jumps from a small input (around +0.025 (Nm)) to a large input (about -0.3 (Nm)) and vice versa. The large input occurs during the stance phase and is used to support the body. The small input occurs during the swing phase and is used only to move the swing leg forward.

Fig. 5 (b) shows the consumed energy of the motors. The red solid line is the absolute consumed energy. It is assumed that the motors cannot regenerate energy using external work. The blue dashed line is the energy. It is assumed that the motors can regenerate the energy in this case. The two lines are almost the same. From Fig. 4, the biped walks 20 steps in 10 (s), and the average consumed energy is about 0.2 (J) per step. The generated energy is about 4.0 (J) for 20 steps, and it is almost equivalent to the provided energy in Fig. 4. Thus, we can see that the control method is very efficient.

B. In the case of a four-link biped with a mass body

Fig. 6 shows the four-link planar biped with a mass body. The center of mass of the upper body is at the hip joint. The range of motion of the knee joints is limited to the range between 0 and π (rad), where the knee angle is 0 when the leg is straight. During the swing phase, the biped starts

TABLE I

LINK PARAMETERS OF A SIMPLE BIPED.

parameter	value	(unit)
m_H	2.000	(kg)
m_L	0.125	(kg)
a	0.200	(m)
b	0.200	(m)

TABLE II

LINK PARAMETERS OF A FOUR-LINK BIPED WITH A MASS BODY.

parameter	value	(unit)
m_0	2.000	(kg)
m_1	0.300	(kg)
m_2	0.200	(kg)
l_1	0.200	(m)
l_2	0.200	(m)
l_{g1}	0.160	(m)
l_{g2}	0.120	(m)

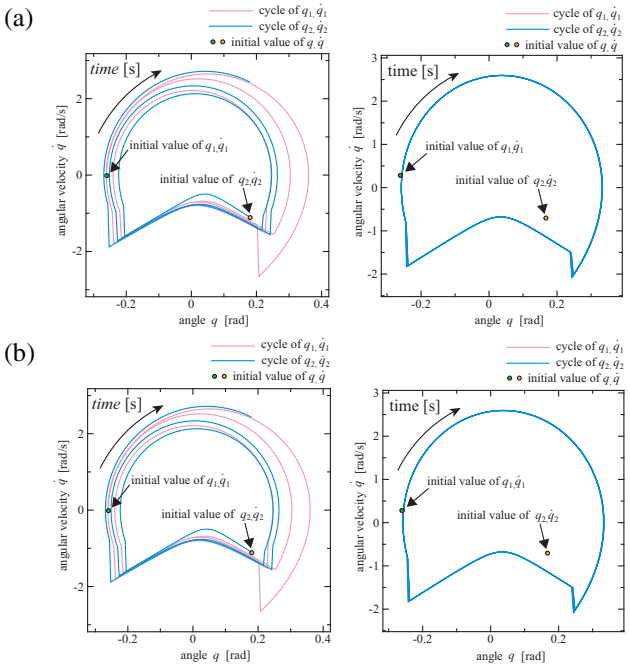

Fig. 3. Phase diagram of unpowered and powered simple bipeds. (a) the unpowered, (b) the powered. The left and the right figures show the transit and steady state motions, respectively.

bending the knees. The biped keeps straightening the knees after the knee reaches an outer bound of its range of motion.

In this section, we compared the unpowered biped and the powered biped as shown in section IV-A. We also show a simulation on an ideal slope which descends from 0 (rad) to -0.045 (rad).

First, we consider the unpowered biped. Fig.7 (a) shows the phase graph of the hip joint when the slope is $\alpha = -0.03$ (rad). The left and the right graphs are the transition period and the steady states, respectively. The circles in the figure are the initial states. The upper and lower arcs are the swing and stance phases, respectively. The sharp edge in the middle

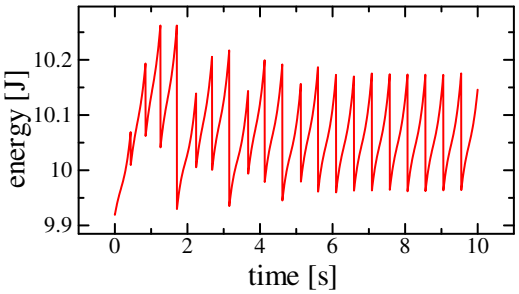

Fig. 4. The whole energy of the unpowered simple biped

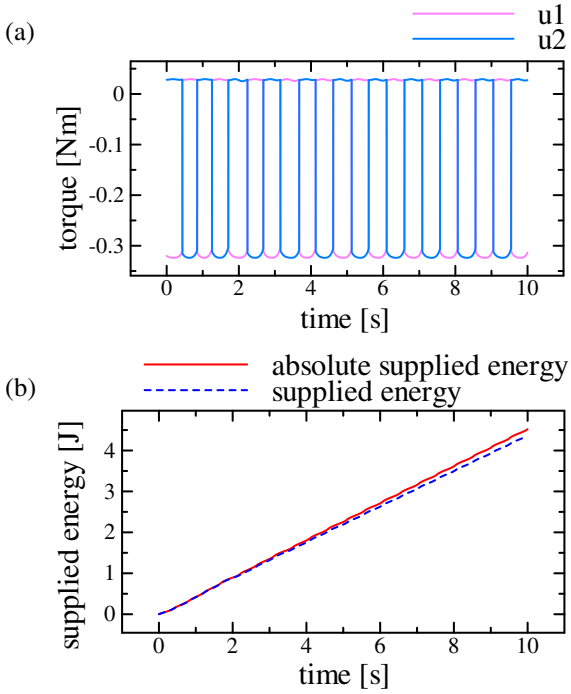

Fig. 5. The control input and the supplied energy of the powered simple biped; (a) the control inputs of the hip joints, (b) the energy supplied by the actuators.

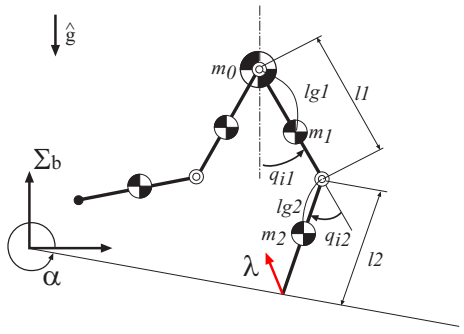

Fig. 6. four-link biped with a mass body

of the swing phase is caused by the collision of the knee. The knee velocity becomes small and recovers instantaneously because the shin is rotating in the opposite direction of the thigh, but the translational motion of both the shin and the thigh are in the same direction. Thus, the swing leg does not

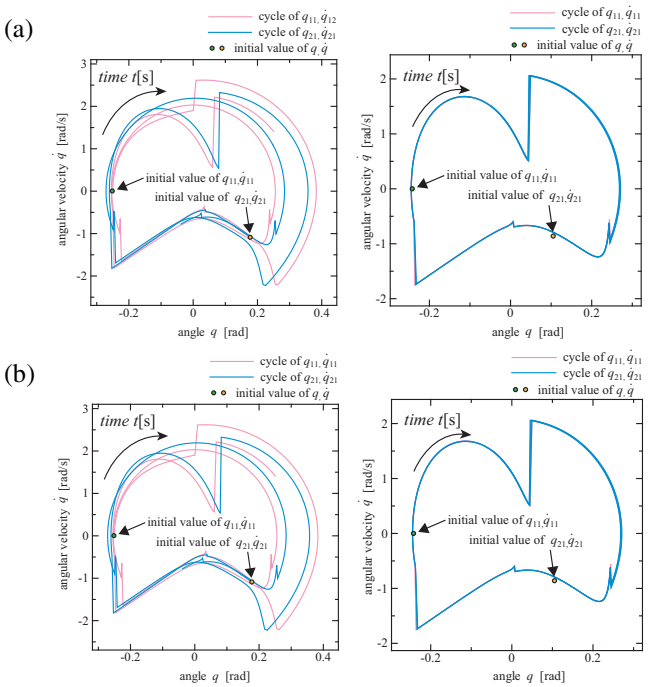

Fig. 7. Phase diagram of unpowered and powered four-link bipeds with a mass body. (a) unpowered, (b) powered. The left and the right figures show the transit and steady state motions, respectively.

lose much energy. In the steady state, the trajectories of both legs are almost the same, and the walking pattern becomes stable.

Fig. 7 (b) shows the phase graph of the powered biped, where $\alpha = 0.00$ (rad) and $\beta = -0.03$ (rad). The graph is almost the same as the one in Fig. 7 (a), and the proposed control method is also effective when the number of the joints is increased.

Fig. 8 is the total energy of the unpowered biped. The energy repeats the same pattern so that the stable walking of the biped was confirmed. The loss of energy at about 9.80 (J) and 9.85 (J) is due to the collisions of the knee and the foot, respectively. Energy is recovered by the gravitational force. Fig. 9 (a) and (b) show the hip and knee control inputs. The hip input is almost the same as that of the compass-like biped, and the knee joint is driven only during the swing phase until the knee collision. The inputs do not diverge at the singularities. Fig. 9 (c) shows the supplied energy of the motors, where the red solid line is the absolute energy, and the blue dashed line is the energy that is allowed to recover. These two lines are almost the same.

From Fig. 8, the biped takes about 19 steps during 10 (s), and the consumed energy is about 0.16(J) per step; thus, the system uses about 3 (J) for 10 (s). As for the compass-like biped, the consumed power of the motor is almost the same as the consumed energy. Thus, the control method is very efficient.

Finally, we investigate the behavior of the four-link biped with a mass body on a slope that was changed continuously. The controller-generated virtual gravity forces the robot to

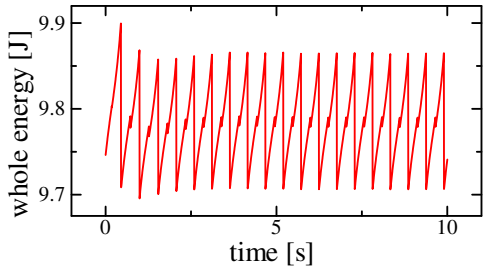

Fig. 8. The whole energy of the four-link powered biped with a mass body

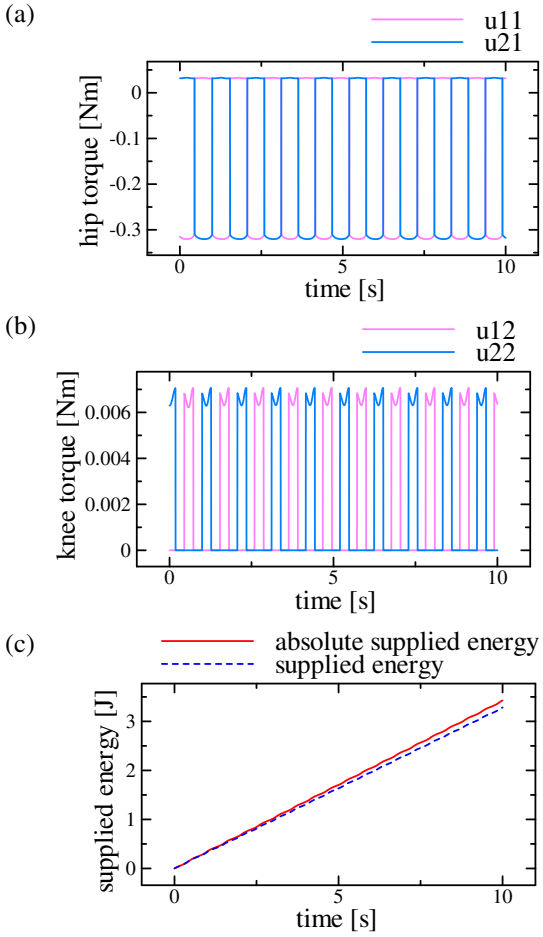

Fig. 9. The control input and the supplied energy of the four-link powered biped with a mass body; (a) the control inputs of the hip joints, (b) the control inputs of the knee joints, (c) the energy supplied by the actuators.

realize walking dynamics as if on the ideal constant slope. Fig. 10 (a) and (b) show the control input of the hip and knee joints. Fig. 10 (c) shows the energy consumption of the motors, where the blue dashed and the red solid lines are supplied and absolute supplied energy by the motors, respectively. The angle of the slope coincides with the desired one at 15 (s). The control inputs becomes smaller as the slope approaches the ideal value and becomes larger as deviations between the actual and the ideal slopes increase. The shape of the control inputs are almost symmetric about the point where the ideal and the actual slope angles are the same.

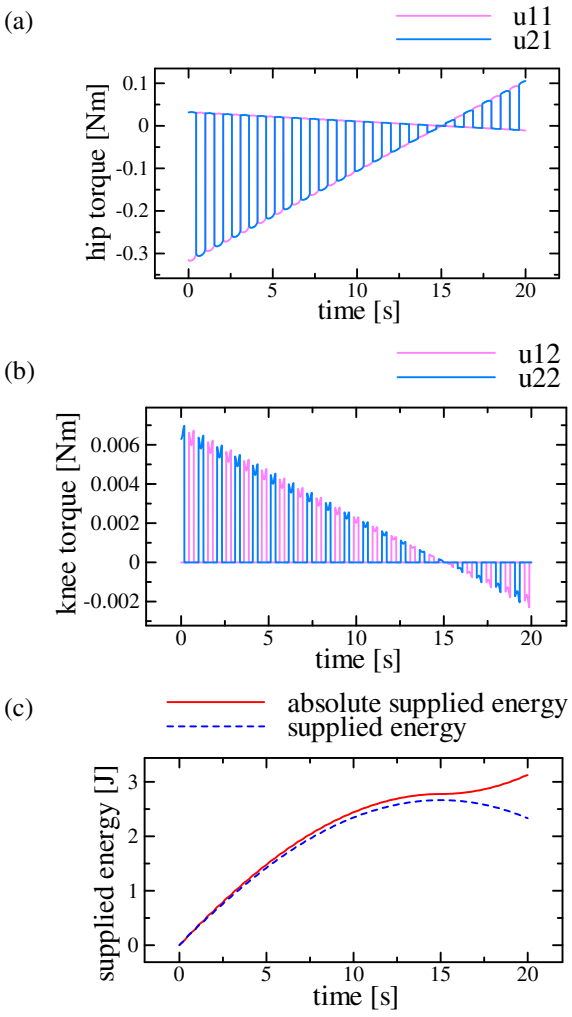

Fig. 10. The control input and the supplied energy of the four-link powered biped with a mass body on a uneven ground. (a) the control inputs of the hip joints, (b) the control inputs of the knee joints, (c) the energy supplied by the actuators.

However, the shape of the consumed energy is not symmetric. The incline of the supplied energy becomes zero at 15 (s), but the supplied and the absolute supplied energies diverge after 15 (s). This is because the consumed energy is recovered when the actual slope is much larger than the ideal one. On the other hand, the motors are used to suppress the gravitational force when the motors cannot regenerate the energy; thus, the energy efficiency is poor compared to the case in which energy recovery is allowed.

V. Conclusion

In this paper, under the assumption that there is an ideal slope on which unpowered bipeds can walk, we designed a virtual gravity controller for a planar biped robot without ankle actuation on various ground, as if it walks on the ideal slope. The lack of ankle actuation makes it difficult to compensate gravitational forces acted on the upper body. However, the proposed controller for a stance leg was refined to compensate these forces without no singular point where the control input diverged, that was often appeared in under-actuated biped controllers.

We demonstrated that the control is equivalent to the control input directly affected on the body. Selected simulations were executed to validate the control method in the case of a simple compass-like biped and a four-link biped with a mass body. The performances of the powered bipeds were almost the same with the unpowered bipeds on an ideal slope. We also executed the simulations in the case that the ground slope was varied over time to show the robustness to the slope change. The proposed control method was effective in this case as well.

Future studies will extend this method to more general cases, such as a three dimensional case and a case where the robot has a multi-link body and feet.

References

[1] T. McGeer. Passive dynamic walking. *The International Journal of Robotics Research*, Vol. 9, No. 2, pp. 62–82, 1990.

[2] A. Goswami, B. Espiau, and A. Keranane. Limit cycles and their stability in a passive bipedal gait. In *Proc. of the 1996 IEEE Inter. Conf. on Robotics and Automation*, pp. 246–251, Minnesota, USA, April 1996.

[3] M. W. Spong. Passivity based control of the compass gait biped. In *Proc. of IFAC world congress*, Beijin, China, July 1999.

[4] F. Asano and M. Yamakita. Virtual gravity and coupling control for robotic gait synthesis. *IEEE Trans. on SMC part A: Systems and Humans*, Vol. 31, No. 6, pp. 737–745, 2001.

[5] A. D. Kuo. Simple model of bipedal walking predicts the preferred speed - step length relationship. *Journal of Biomechanical Engineering*, Vol. 123, pp. 264–269, 2001.

[6] A. D. Kuo. Energetics of actively powered locomotion using simplest walking model. *Journal of Biomechanical Engineering*, Vol. 124, pp. 113–120, 2002.

[7] S. Collins, A. Ruina, R. Tedrake, and M. Wisse. Efficient bipedal robots based on passive-dynamic walkers. *Science*, Vol. 307, pp. 1082–1085, February 2005.

[8] A. Goswami, B. Espiau, and A. Keranane. Limit cycles in a passive gait biped and passivity-mimicking control laws. *Autonomous Robots*, Vol. 4, pp. 273–286, 1997.

[9] M. W. Spong. Controlled symmetries and passive walking. In *Proc. of IFAC World Congress*, Barcelona, Spain, July 2002.

[10] J. Perry. *Gait analysis*. Slack Inc., Thorofare, NJ, 1992.

[11] S. H. Collins, M. Wisse, and A. Ruina. A three-dimensional passive-dynamic walking robot with two legs and knees. *The International Journal of Robotics Research*, Vol. 20, No. 7, pp. 607–615, 2001.

[12] R. Q. van der Linde. Passive bipedal walking with phasic muscle contraction. *Biological Cybernetics*, Vol. 81, No. 3, pp. 227–237, 1999.

[13] M. Wisse, J. V. Feliksdal, G. Frankenhuyzen, and B. Moyer. Passive-based walking robot. *IEEE Robotics and Automation Magazine*, Vol. 14, No. 2, pp. 52–62, 2007.

[14] C. Chevallereau, G. Abba, Y. Aoustin, E. R. Plestan, F. Westervelt, C. Canudas-de Wit, and J. W. Grizzle. Rabbit: A testbed for advanced control theory. *IEEE Control Systems Magazine*, Vol. 23, No. 5, pp. 57–79, 2003.

[15] A. Goswami, B. Espiau, F. Keramane, and F. Genot. The gait of a compass-like biped robot: limit cycles, passive stability, and active control. Technical report, INRIA, 1995.

[16] Y. Hurmuzlu, F. Genot, and B. Brogliato. Modeling, stability and control of biped robots - a general framework. *Automatica*, Vol. 40, pp. 1647–1664, 2004.